Original Article
Yonsei Med J 2021 Jun;62(6):535-544
https://doi.org/10.3349/ymj.2021.62.6.535
Yonsei Medical Journal
YMJ
pISSN: 0513-5796 · eISSN: 1976-2437

DNM3OS Facilitates Ovarian Cancer Progression by Regulating miR-193a-3p/MAP3K3 Axis

Lei He and Guolin He

Department of Gynecology and Obstetrics, Key Laboratory of Obstetrics and Gynecologic and Pediatric Diseases and Birth Defects of Ministry of Education, West China Second Hospital, Sichuan University, Chengdu, China.

Purpose: Long non-coding RNAs (lncRNAs) are essential regulators in the development of ovarian cancer (OC). Nonetheless, the function of lncRNA DNM3 opposite strand/antisense RNA (DNM3OS) in OC remains unclear. This work aimed to investigate the biological roles and underlying mechanisms of DNM3OS in OC.

Materials and Methods: Quantitative real-time polymerase chain reaction was conducted to examine DNM3OS, microRNA (miR)-193a-3p, and mitogen-activated protein kinase 3 (MAP3K3) mRNA expression in OC tissues and cell lines. Kaplan-Meier survival analysis was employed to analyze the relationship between DNM3OS expression and the prognosis of OC patients. Cell counting kit-8, 5-ethynyl-2'-deoxyuridine, and transwell experiments were conducted to monitor cell proliferation, migration, and invasion, respectively. Western blot was applied to examine epithelial-mesenchymal transition associated protein (E-cadherin and N-cadherin) expression. Luciferase reporter gene and RNA immunoprecipitation experiments were performed to confirm the relationships among DNM3OS, miR-193a-3p, and MAP3K3. Pearson's correlation analysis was adopted to analyze the correlations among DNM3OS, miR-193a-3p, and MAP3K3 mRNA.

Results: DNM3OS expression was remarkably increased in OC tissues and cell lines, which was associated with the unfavorable prognosis of the patients. DNM3OS overexpression enhanced OC cell proliferation, migration, and invasion; suppressed E-cadherin protein expression; and facilitated N-cadherin protein expression, while the transfection of miR-193a-3p mimics had the opposite effects. DNM3OS directly interacted with miR-193a-3p, and miR-193a-3p targeted MAP3K3 by directly binding to 3'UTR. DNM3OS could up-regulate the expression of MAP3K3 via repressing miR-193a-3p expression.

Conclusion: DNM3OS, as an oncogenic lncRNA, increases the malignancy of OC cells via regulation of an miR-193a-3p/MAP3K3 axis.

Key Words: lncRNA, DNM3OS, miR-193a-3p, MAP3K3, ovarian cancer

INTRODUCTION

Ovarian cancer (OC) is the second most common gynecologic cancer worldwide and is one of the leading causes of cancer-related death among women.[1-3] Despite great progress in the treatment of OC, the prognosis of OC patients, especially for those who present with metastasis or drug resistance, is still adverse.[3] Hence, it is of great significance to explore the molecular mechanisms of OC progression and to find novel targets for effective treatment.[4,5]

Long non-coding RNAs (lncRNAs) are aberrantly expressed in diverse tumors and are implicated in tumorigenesis and cancer progression.[6-8] For instance, LINC00339, lncRNA UCA1, and lncRNA GAS5 are all aberrantly expressed in OC and participate in biological processes, such as cell proliferation, differentiation, and apoptosis.[9-11] DNM3 opposite strand/antisense RNA (DNM3OS) is a lncRNA encoded by an independent transcription unit that is located on chromosome 1 and is embedded in the intron of the Dynamin 3 gene.[12] DNM3OS partakes in diverse biological processes.[13-16] For instance, DNM3OS

Received: July 31, 2020 **Revised:** January 8, 2021
Accepted: February 9, 2021
Corresponding author: Guolin He, PhD, Department of Gynecology and Obstetrics, Key Laboratory of Obstetrics and Gynecologic and Pediatric Diseases and Birth Defects of Ministry of Education, West China Second Hospital, Sichuan University, Chenglong Road Section 1 No.1416, Jinjiang District, Chengdu 610000, Sichuan, China.
Tel: 86-028-88570307, Fax: 86-028-88570717, E-mail: sujieba31@163.com

•The authors have no potential conflicts of interest to disclose.

enhances radioresistance of esophageal squamous cell carcinoma cells by regulating the DNA damage response.[14] In oral cancer, DNM3OS facilitates tumor growth and metastasis via modulating a microRNA (miR)-204-5p/HIP1 molecular axis.[15] Research has shown that DNM3OS expression is up-regulated in OC and that its high expression is significantly associated with shorter overall survival. While knocking down DNM3OS suppressed OC cell migration and invasion,[16] the specific mechanism thereof is still largely unknown.

Reportedly, microRNA (miR)-193a-3p expression is down-regulated in OC, and miR-193a-3p inhibits tumor growth.[17] Moreover, mitogen-activated protein 3 kinase 3 (MAP3K3) expression is up-regulated in OC, and MAP3K3 enhances OC proliferation and metastasis.[18] Interestingly, bioinformatics analysis suggests that MAP3K3 is a potential target gene of miR-193a-3p and that miR-193a-3p may be adsorbed by DNM3OS. We supposed that DNM3OS could probably facilitate OC progression through regulating a miR-193a-3p/MAP3K3 axis. This study was designed to validate this scientific hypothesis.

MATERIALS AND METHODS

Clinical specimens

The study was endorsed by the Ethics Committees of the West China Second University Hospital (Approval number: 2015-02). OC tissues (n=49) and para-carcinoma tissues (n=18) in this study were obtained from the Tissue Bank of West China Second University Hospital. The para-carcinoma tissues were obtained from the tissues >2 cm from the margin of the tumor tissues. None of the patients had received preoperative radiotherapy or chemotherapy, and informed consent had been signed by the patients prior to specimen collection. The procedures of human sample collection and use were performed with principles of the Declaration of Helsinki.

Cell culture and transfection

OC cell lines (HO8910PM, SKOV3, A2780, ES2, and HO8910 cells) and human normal ovarian epithelial cells IOSE-80 were obtained from the China Center for Type Culture Collection (CCTCC, Wuhan, China). Cells were cultured in Dulbecco's Modified Eagle's Medium (DMEM, Gibco, Carlsbad, CA, USA) containing 10% fetal bovine serum (FBS, Gibco, Carlsbad, CA, USA), 100 U/mL penicillin, and 100 μg/mL streptomycin (Gibco, Grand Island, NY, USA) at 37°C with 5% CO_2. The medium was changed every 3 days, and subculture was performed when the cells grew to about 80% confluence. The cells in logarithmic growth phase were harvested for subsequent experiments.

MiR-193a-3p mimics (sequence: 5'-AACUGGCCUACAAAGUCCCAGU-3'), mimics normal control (miR-NC, sequence: 5'-UUCUCCGAACGUGUCACGUTT-3'), miR-193a-3p inhibitors (sequence: 5'-ACUGGGACUUUGUAGGCCAGUU-3'), inhibitor negative control (inh-NC, sequence: 5'-ACGUGACACGUUCGGAGAATT-3'), two different shRNAs targeting DNM3OS (sh-DNM3OS#1, sequence: 5'-GCCAACACATTCACTTGCA-3' and sh-DNM3OS#2, sequence: 5'-CCAACACATTCACTTGCAA-3'), negative control shRNA (sh-NC, sequence: 5'-GCCCACTTACACTTAAGCA-3'), DNM3OS overexpression plasmid, and empty control vector (NC) were synthesized by GenePharma (Shanghai, China). Transfection was performed using Lipofectamine™ 2000 (Invitrogen, Carlsbad, CA, USA) following the manufacturer's instructions. Quantitative real-time polymerase chain reaction (qRT-PCR) was applied to detect DNM3OS or miR-193a-3p expression after 24 h to determine the transfection efficiency.

qRT-PCR

The extraction of total RNA from cells was performed using TRIzol reagent (ComWin Biotech, Beijing, China), and cDNA was generated using TransScript First-Strand cDNA Synthesis SuperMix (TransGen Biotech, Beijing, China). With the cDNA as a template, qRT-PCR was carried out using SYBR® Premix-Ex-Taq™ (Takara, Tokyo, Japan) on an ABI 7500 Fast Real-Time PCR System (Applied Biosystems, Foster City, CA, USA). For quantifying miR-193a-3p, U6 was used as an internal reference; for quantifying DNM3OS and MAP3K3, GAPDH was used as an internal reference. The $2^{-\Delta\Delta Ct}$ method was adopted to make the relative quantification of the genes. The primer sequences are listed in Table 1.

Cell counting kit-8 experiment

SKOV3 and A2780 cells in logarithmic growth phase were trypsinized, transferred into 96-well plates at a density of 2×10^3 cells/well, and cultured for 1, 2, and 3 d, respectively. On each day, 10 μL of cell counting kit-8 (CCK-8) solution (Dojindo, Kumamoto, Japan) was supplemented into each well, and the cell culture was continued for 2 h. Afterwards, the absorbance at 450 nm of each group of cells was detected on a microplate reader. Three days later, the proliferation curve was plotted based on the absorbance values.

Table 1. The Primers Used in this Study

Name	Primer sequence
DNM3OS	Forward: GTCAGGCGTTCTCGTCTC
	Reverse: CACCACATCGATCACGAAGA
miR-193a-3p	Forward: ACTGGCCTACAAAGTCCCAGT
	Reverse: GTGCAGGGTCCGAGGT
MAP3K3	Forward: CGAAAGTACACGCGGCAGAT
	Reverse: CAGCAGAGTCTCGGAGGATGTT
U6	Forward: GCTTCGGCAGCACATATACTAA
	Reverse: AACGCTTCACGAATTTGCGT
GAPDH	Forward: TGGACTCCACGACGTACTCAG
	Reverse: CGGGAAGCTTGTCATCAATGGAA

https://doi.org/10.3349/ymj.2021.62.6.535

Transwell experiment

In the migration assay, the density of OC cell suspensions was modulated to 1×10^5 cells/mL with serum-free medium. A total of 200 μL of cell suspension was supplemented to the upper compartment of each transwell chamber (pore size: 8 μM; Corning, NY, USA), and 600 μL of medium containing 10% FBS was added to the lower compartment. The cells were cultured for 12 h, and then, the cells that did not pass through the membrane were removed with cotton swabs. The migrated cells were fixed with 4% paraformaldehyde and stained with 0.1% crystal violet solution, followed by being washed, dried, photographed, and counted. The procedures for the invasion assay were the same as those for the migration assay, except that the membranes of the transwell chambers were precoated with Matrigel (30 μg/well; BD Biosciences, San Jose, CA, USA) before the cells were inoculated.

5-Ethynyl-2'-deoxyuridine experiment

The transfected SKOV3 and A2780 cells were transferred into 24-well plates and cultured for 24 h. Then 5-ethynyl-2'-deoxyuridine (EdU) assay kit (RiboBio, Guangzhou, China, working concentration: 50 μmol/L) was added to each well, and the cells were incubated for an additional 2 h. Subsequently, the cells were gently rinsed with PBS, fixed with paraformaldehyde for 10 min, and added with glycine (2 mg/mL) before being incubated for 5 min. Afterwards, the cells were washed using PBS on a shaker for 5 min, and 0.5% Triton-X 100 (Sigma, St. Louis, MO, USA) was supplemented to each well. After 10 min, the cells were washed twice with PBS for 5 min each time. The cells were stained with Apollo kits (RiboBio, Guangzhou, China) in the dark for 30 min before DNA was counterstained with DAPI. Ultimately, the images of the cells were collected using a fluorescent microscope.

Western blot

Total protein was extracted from the OC cells using RIPA lysis buffer (Beyotime, Shanghai, China). The concentrations of extracted proteins were determined using the BCA Protein Assay Kit (Beyotime, Shanghai, China). After quantification and denaturation, the protein samples were subjected to SDS-PAGE and then transferred onto a PVDF membrane (pore size: 0.22 μm, BioSharp, Hefei, China). Then, the proteins on the membrane were blocked with 5% skimmed milk for 2 h, and the primary antibodies were added to incubate the membrane overnight at 4°C The next day, the PVDF membrane was washed with TBST, and the secondary antibody was added to incubate the membrane for 1 h at room temperature. After the membranes were washed with TBST again, the protein bands were detected with ECL kits (Servicebio, Wuhan, China) by Amersham Imager 600 (GE Healthcare, Chicago, IL, USA). GAPDH was used as the internal reference. The primary antibodies used in this work, including anti-GAPDH antibody (ab9485, 1:5000), anti-MAP3K3 antibody (ab40756, 1:1000), anti-E-cadherin antibody (ab194982, 1:2000), and anti-N-Cadherin antibody (ab18203, 1:1000), were purchased from Abcam (Shanghai, China).

Dual-luciferase reporter gene experiment

In this study, dual-luciferase reporter vectors were constructed and provided by Promega (Madison, WI, USA). The reporter vectors containing DNM3OS wild-type (WT) sequence and reporter vectors containing DNM3OS mutant (MUT) sequence were co-transfected into HEK-293T cells with miR-193a-3p mimics, miR-193a-3p inhibitors, or negative controls, respectively. After 24 h, the luciferase activity of each group was detected by a dual-luciferase reporter detection system (Promega). The luciferase activity of Firefly was normalized to that of Renilla. The targeting relationship between miR-193a-3p and MAP3K3 was verified with a similar method.

RIP experiment

The EZ-Magna-RIP kit (Millipore, Bedford, MA, USA) was applied for RIP experiments. For Argonaute 2 (Ago2)-based RIP assays, RIP lysis buffer was utilized for lysing the cells. Then, the mixtures were incubated with anti-Ago2 or control anti-immunoglobulin G (IgG) antibodies conjugated with magnetic beads at 4°C for 6 h. After the mixtures were incubated with proteinase K, the RNA was extracted from the immunoprecipitates with TRIzol reagent. Then, qRT-PCR was performed to detect the expressions of DNM3OS and miR-193a-3p.

Bioinformatics analysis

Kaplan-Meier plotter (http://kmplot.com/analysis/index.php) was employed to analyze the relationship between DNM3OS expression and the prognosis of patients. LncBase Predicted v.2 (http://carolina.imis.athena-innovation.gr/) and TargetScan (http://www.targetscan.org/vert_72/) were applied to predict the binding sites between DNM3OS and miR-193a-3p, miR-193a-3p and MAP3K3, respectively.

Statistical analysis

SPSS 20.0 (SPSS Inc., Chicago, IL, USA) was used for analyzing the data, which are presented as a mean±SD. The Shapiro-Wilk normality test was used to assess the normal distribution of the data. Student's t-test was used for making the comparison between the two groups, and one-way ANOVA was used for making the comparison among multiple groups. Pearson's correlation analysis was used for analyzing the correlations among DNM3OS, miR-193a-3p, and MAP3K3. $p<0.05$ was considered statistically significant.

RESULTS

Up-regulation of DNM3OS and MAP3K3 mRNA expression and down-regulation of miR-193a-3p expression in OC tissue samples

First, we detected DNM3OS, miR-193a-3p, and MAP3K3 mRNA expression in 49 cases of OC tissues and 18 cases of adjacent specimens by qRT-PCR. These results showed that DNM3OS and MAP3K3 mRNA expressions were significantly up-regulated in OC tissues relative to those in adjacent tissues, while miR-193a-3p expression was markedly down-regulated (Fig 1A-C). Furthermore, the high expression of DNM3OS was significantly correlated with advanced FIGO stage (Table 2). Survival analysis was performed using the Kaplan-Meier plotter. After the patients were classified into high and low DNM3OS expression groups based on the average value of DNM3OS expression, we noted that high DNM3OS expression was associated with shorter overall survival (OS) and progression-free survival (PFS) in OC patients (Fig. 1D and E).

DNM3OS directly targets miR-193a-3p

Next, we demonstrated that DNM3OS is also overexpressed in OC cell lines, compared with in normal ovarian epithelial IOSE-80 cells (Fig. 2A). Then, the subcellular localization of DNM3OS in SKOV3 and A2780 cells was detected using qRT-PCR, after RNA from the nucleus and cytoplasm was extracted. The data implied that DNM3OS is predominantly distributed in the cytoplasm of OC cells (Fig. 2B), suggesting that it might function as a competitive endogenous RNA (ceRNA). The online bioinformatics analysis tool LncBase Predicted v.2 predicted that there were two potential binding sites for miR-193a-3p in the sequence of DNM3OS (Fig. 2C). To validate the targeting relationship between DNM3OS and miR-193a-3p, dual-luciferase reporter experiments were carried out. The results thereof indicated that, compared with the control group, miR-193a-3p overexpression decreased the luciferase activity of the DNM3OS-WT reporter vector, but did not influence that of the DNM3OS-MUT reporter, while miR-193a-3p inhibitors increased the luciferase activity of the DNM3OS-WT reporter vector, but exerted no effect on that of the DNM3OS-MUT reporter (Fig 2D). Moreover, we found that miR-193a-3p expression in OC tissues was negatively correlated with DNM3OS expression by Pearson's correlation analysis (Fig. 2E). Subsequently, we transfected DNM3OS overexpression plasmids into SKOV3 cells and transfected sh-DNM3OS#1 and sh-DNM3OS#2 into A2780 cells (Fig. 2F). RIP assay revealed that DNM3OS and miR-193a-3p were remarkably enriched in Ago2 immunoprecipitates relative to the IgG-pellet (Fig. 2G). Moreover, DNM3OS overexpression decreased miR-193a-3p expression in SKOV3 cells, while DNM3OS knockdown increased miR-193a-3p expression in A2780 cells (Fig. 2H). Collectively, these results suggested that DNM3OS is a molecular sponge for miR-193a-3p to repress its expression.

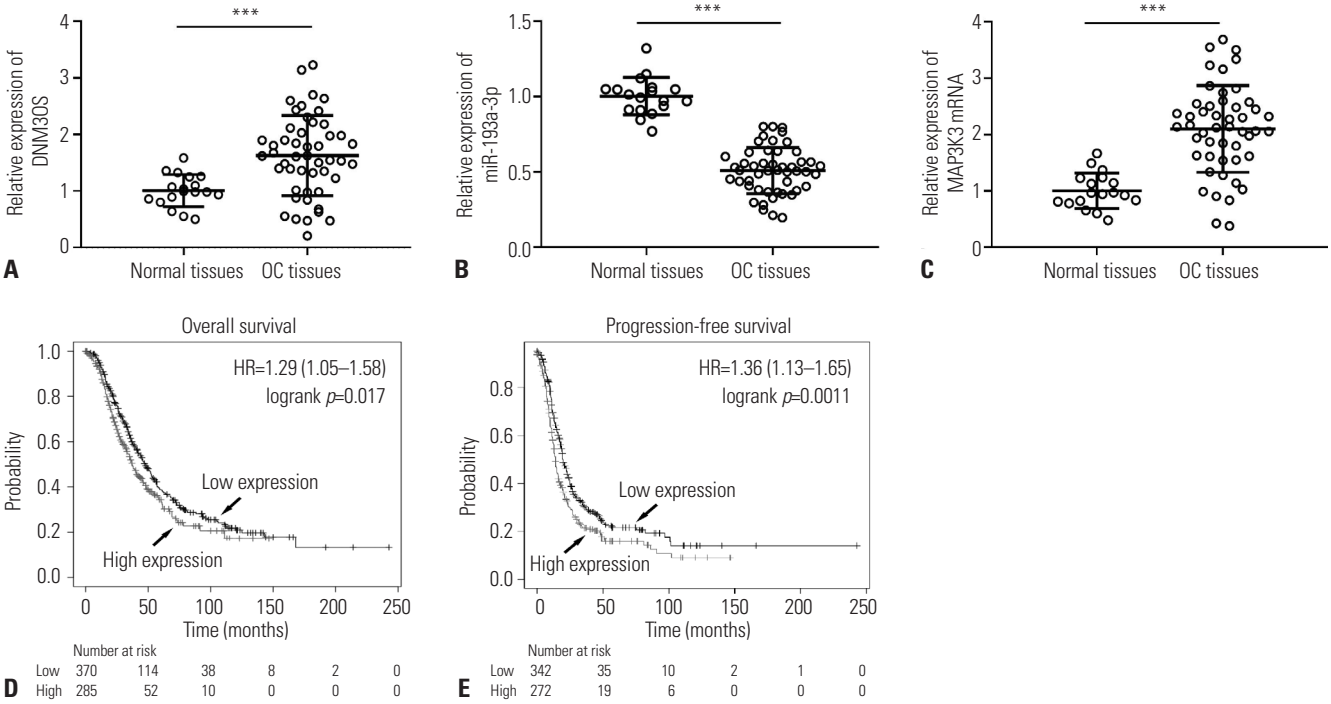

Fig. 1. The expressions of DNM3OS, miR-193a-3p, and MAP3K3 in OC. (A-C) The expressions of DNM3OS, miR-193a-3p, and MAP3K3 mRNA in 49 OC tissues and 18 normal ovarian tissues were determined by qRT-PCR. (D and E) The Kaplan-Meier plotter database was used to analyze the relationship between DNM3OS expression and the prognosis of OC patients. ***$p<0.001$. OC, ovarian cancer.

https://doi.org/10.3349/ymj.2021.62.6.535

Table 2. Correlation between Clinicopathological Features and Expression of DNM3OS in Ovarian Cancer

Feature	All patients (n)	DNM3OS expression level		Chi-square value	*p* value
		High expression	Low expression		
All patients	49	25	24		
Age				3.496	0.062
≥50 yr	23	15	8		
<50 yr	26	10	16		
Histological type				0.164	0.922
Serous	15	8	7		
Endometrioid	17	9	8		
Mucous or others	17	8	9		
FIGO stage				4.601	0.032*
I/II	21	7	14		
III/IV	28	18	10		
Degree of differentiation				1.634	0.201
Poor	27	16	11		
High, moderate	22	9	13		

*$p<0.05$.

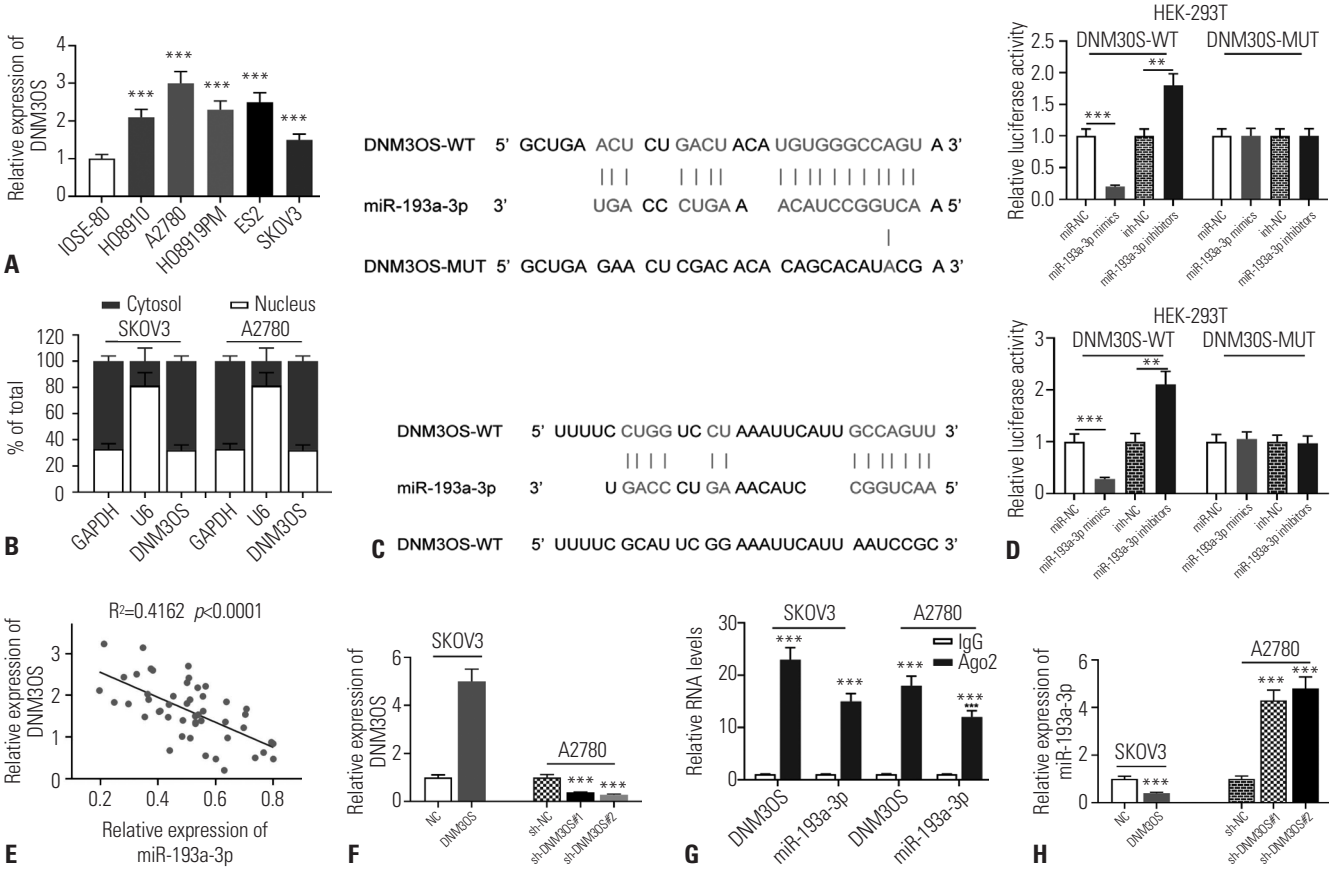

Fig. 2. DNM3OS directly targets miR-193a-3p. (A) The expression of DNM3OS in OC cell lines and human normal ovarian epithelial IOSE-80 cells was detected by qRT-PCR. (B) The subcellular localization of DNM3OS in SKOV3 and A2780 cells. (C) The online database LncBase Predicted v.2 was used to predict the binding sites between DNM3OS and miR-193a-3p. (D) The DNM3OS-WT luciferase reporter vector or DNM3OS-MUT luciferase reporter vector was co-transfected with miR-193a-3p mimics or miR-193a-3p inhibitors into HEK-293T cells, and the luciferase activity was measured. (E) Pearson's correlation analysis was used to analyze the correlation between DNM3OS expression and miR-193a-3p expression in OC samples. (F) OC cells were transfected with DNM3OS shRNAs or DNM3OS overexpression plasmid, and qRT-PCR was used to determine the transfection efficiency. (G) The interaction between DNM3OS and miR-193a-3p was analyzed by RIP experiments. (H) qRT-PCR was used to detect the effects of overexpression or knockdown of DNM3OS on miR-193a-3p expression in OC cells. **$p<0.01$, ***$p<0.001$. OC, ovarian cancer.

Effects of DNM3OS and miR-193a-3p on OC cell proliferation

To expound on the biological function of DNM3OS in OC cells, SKOV3 cells were co-transfected with DNM3OS overexpression plasmid and miR-193a-3p mimics; A2780 cells were co-transfected with sh-DNM3OS#2 and miR-193a-3p inhibitors. qRT-PCR data verified that the transfection was successful (Fig. 3A). The proliferation of these two cell lines was assessed using CCK-8 and EdU experiments, and the results showed that, compared with the NC group, the proliferation of SKOV3 cells was markedly promoted after DNM3OS was overexpressed, while miR-193a-3p mimics partly abolished this effect. Compared with sh-NC group, the proliferation of A2780 cells was remarkably decreased after DNM3OS was knocked down, while miR-193a-3p inhibitors reversed such effects (Fig 3B and C).

Effects of DNM3OS and miR-193a-3p on cell migration and invasion

Transwell experiments were employed to examine the effects of DNM3OS and miR-193a-3p on OC cell migration and invasion. The results demonstrated that, compared with NC group, the migration and invasion of SKOV3 cells were markedly increased after DNM3OS was overexpressed, while the co-transfection of miR-193a-3p mimics suppressed these effects. Compared with the sh-NC group, the migration and invasion of A2780 cells were remarkably decreased after DNM3OS was silenced, while miR-193a-3p inhibitors reversed such effects (Fig. 4A). Subsequently, Western blot was performed to examine expressions of epithelial mesenchymal transition (EMT)-related proteins, including E-cadherin and N-cadherin. The results revealed that DNM3OS overexpression enhanced N-cadherin expression and impeded E-cadherin expression in SKOV3 cells, and miR-193a-3p mimics attenuated these effects. Knocking down DNM3OS repressed N-cadherin expression and promoted E-cadherin expression, while the co-transfection of miR-193a-3p inhibitors counteracted these effects (Fig. 4B). These data further indicate that DNM3OS/miR-193a-3p regulates the malignant biological behaviors of OC cells.

DNM3OS regulates MAP3K3 expression by competitively binding to miR-193a-3p

Accumulating research has shown that MAP3K3 functions as an oncogene in diverse cancers, but its upstream mechanism in OC remains unclear. The TargetScan database suggested that the 3'-UTR of MAP3K3 had a binding site for miR-193a-3p (Fig. 5A). Hence, we constructed MAP3K3-WT and MAP3K3-MUT dual-luciferase reporter vectors, and dual-luciferase reporter gene experiments were performed (Fig. 5B). The results indicated that miR-193a-3p mimics reduced the luciferase activity of the MAP3K3-WT reporter vector, while miR-193a-3p inhibitors elicited the opposite effect. However, neither miR-193a-3p mimics nor miR-193a-3p inhibitors had a significant effect on the luciferase activity of the MAP3K3-MUT reporter

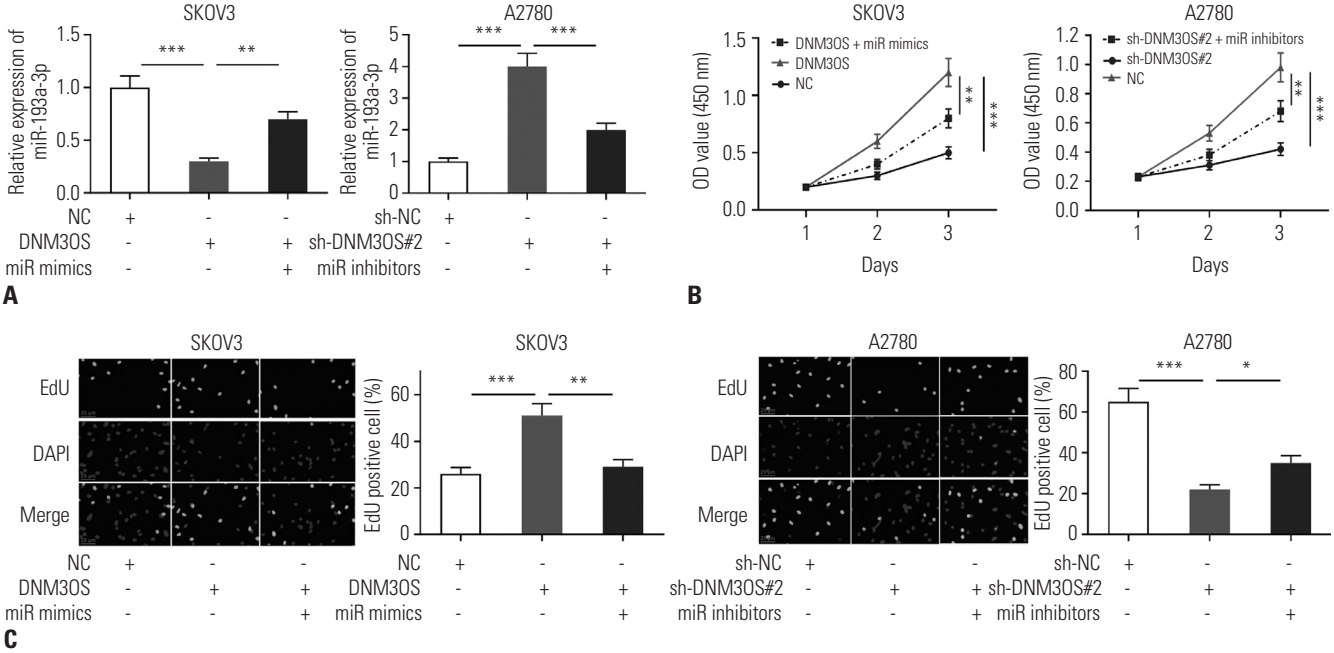

Fig. 3. The effects of DNM3OS/miR-193a-3p axis on OC cell proliferation. (A) DNM3OS overexpression plasmid and miR-193a-3p mimics were co-transfected into SKOV3 cells, and sh-DNM3OS#2 and miR-193a-3p inhibitors were co-transfected into A2780 cells. qRT-PCR was used to detect the expression of miR-193a-3p. (B) The effects of DNM3OS and miR-193a-3p on the proliferation of SKOV3 and A2780 cells were detected using the CCK-8 method. (C) EdU experiments were used to detect the effects of DNM3OS and miR-193a-3p on the proliferation of SKOV3 and A2780 cells. *p<0.05, **p<0.01, ***p<0.001. OC, ovarian cancer.

https://doi.org/10.3349/ymj.2021.62.6.535

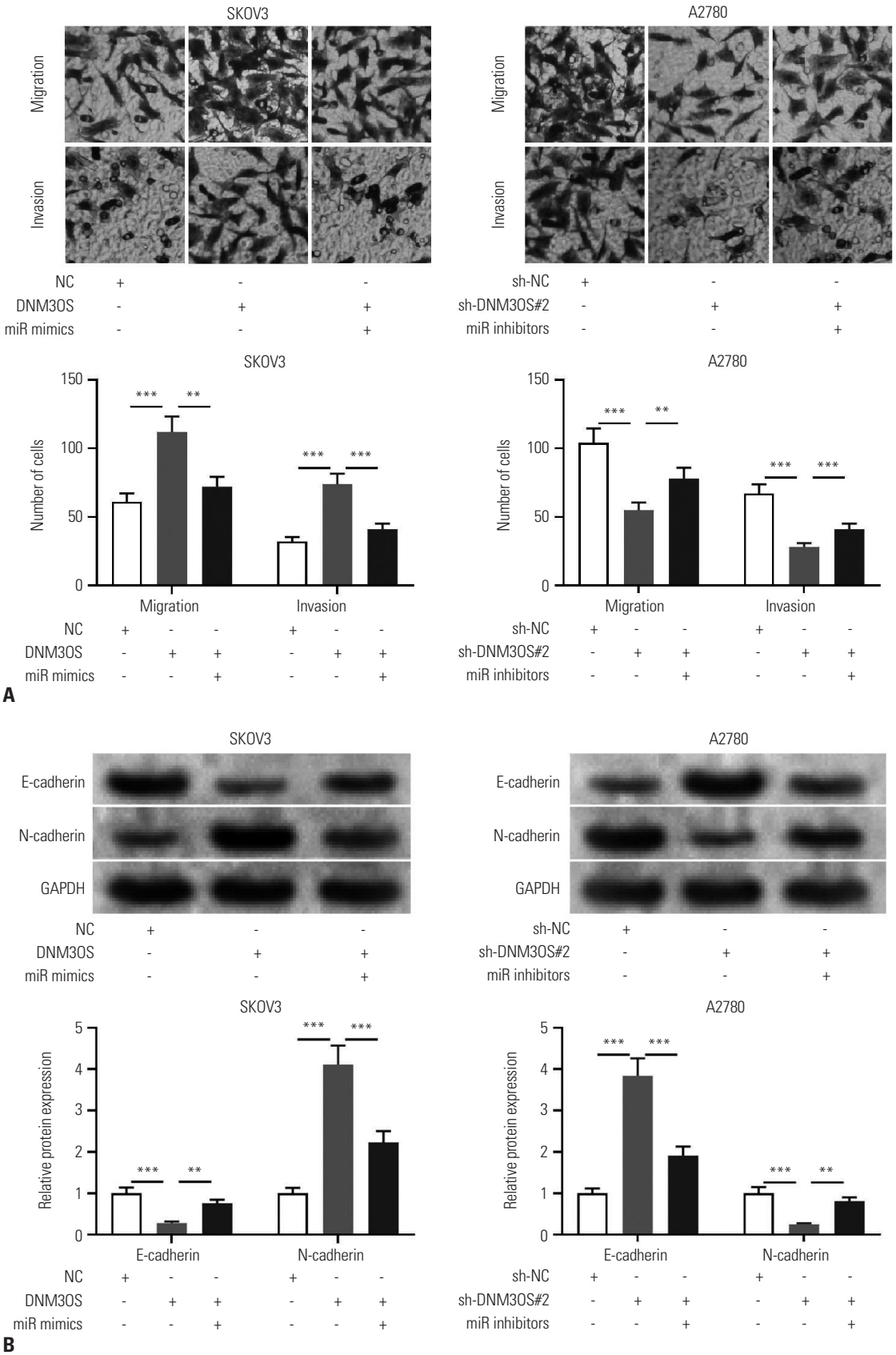

Fig. 4. The effects of the DNM3OS/miR-193a-3p axis on OC cell migration, invasion, and EMT process. (A) Transwell experiments were used to detect the effects of DNM3OS and miR-193a-3p on SKOV3 and A2780 cell migration and invasion. (B) Western blot was used to detect the effects of DNM3OS and miR-193a-3p on the expressions of E-cadherin and N-cadherin in OC cells. **p<0.01, ***p<0.001. OC, ovarian cancer.

(Fig. 5C). Additionally, miR-193a-3p expression was negatively correlated with MAP3K3 mRNA expression in OC samples (Fig. 5D). Western blot showed that DNM3OS overexpression enhanced MAP3K3 expression, while the co-transfection of miR-193a-3p mimics abrogated this effect. Conversely, knockdown of DNM3OS restrained MAP3K3 expression, while miR-193a-3p inhibitors reversed it (Fig. 5E). Pearson's correlation analysis showed a positive correlation between DNM3OS expression and MAP3K3 mRNA expression in OC samples (Fig. 5F).

DISCUSSION

Recent research has revealed that multiple lncRNAs are involved in OC progression. For example, lncRNA ATB and UBC1 are abnormally highly expressed in OC and predict an unfavorable prognosis in OC patients. Both of them have been found to enhance the proliferation, migration, and invasion of OC cells and to impede apoptosis.[19,20] LncRNA MALAT1 enhances OC cell stemness by inhibiting YAP translocation from the nucleus to cytoplasm.[21] LncRNA SNGH7 is activated by SP1 and accelerates OC progression by interacting with EZH2.[22] Meanwhile, DNM3OS has been found to participate in diverse biological processes, such as cell differentiation, cell growth, tumorigenesis, and so on.[23,24] Reportedly, DNM3OS facilitates retinoblastoma progression via modulating the miR-134-5p/SMAD6 molecular axis.[25] In gastric cancer, knockdown of DNM3OS restrains cancer cell migration and invasion via suppressing Snail-mediated EMT.[26] In OC, DNM3OS expression is reported to be up-regulated and its high expression predicts a poor prognosis. Additionally, knockdown of DNM3OS results in altered EMT-related genes/pathways, and reduces OC cell migration and invasion,[16] which is similar to the results of the present

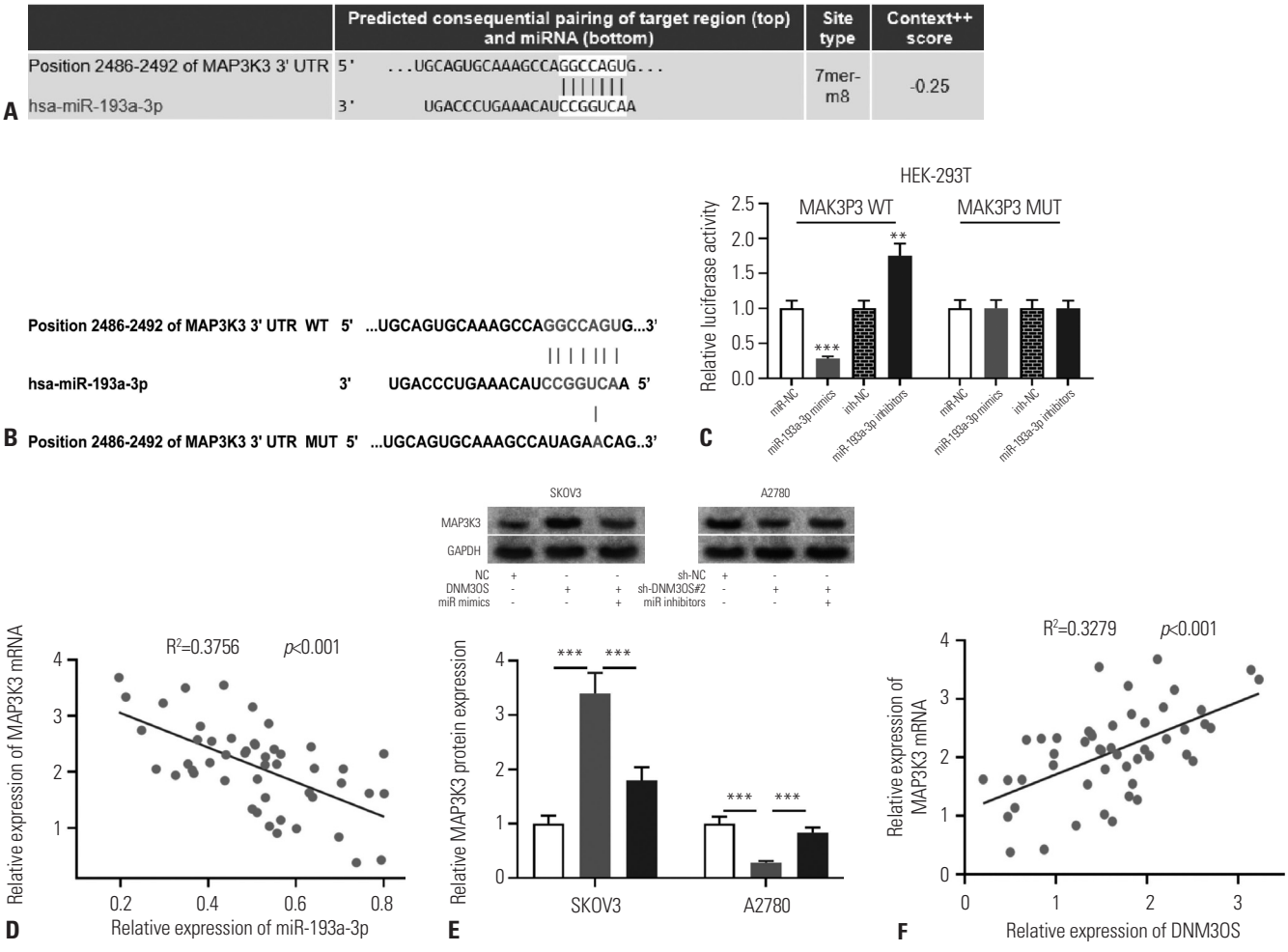

Fig. 5. DNM3OS up-regulates MAP3K3 expression by adsorbing miR-193a-3p. (A) The TargetScan database was used to predict binding sites between the 3'UTR of MAP3K3 and miR-193a-3p. (B) MAP3K3 WT and MUT dual-luciferase reporter vectors were constructed. (C) Dual-luciferase reporter assay was employed to validate the targeting relationship between the 3'UTR of MAP3K3 and miR-193a-3p. (D) Pearson's correlation analysis was performed to assess the association between the expressions of miR-193a-3p and MAP3K3 mRNA in OC tissues. (E) Western blot was used to detect the effects of DNM3OS and miR-193a-3p on MAP3K3 expression. (F) Pearson's correlation analysis was performed to assess the association between the expressions of DNM3OS and MAP3K3 mRNA in OC tissues. **p<0.01, ***p<0.001. OC, ovarian cancer.

https://doi.org/10.3349/ymj.2021.62.6.535

study. Overall, our work supports DNM3OS as an oncogenic lncRNA in OC and as a promising biomarker and therapy target for the diagnosis and treatment of OC.

MiRNAs are highly conserved, small (about 22 nucleotides in length), single-stranded non-coding RNAs.[27] Previous research has shown that miRNAs are closely related to tumor growth, metastasis, and cancer progression.[28] MiR-193a-3p has been identified as a tumor suppressor. For instance, it is reported that miR-193a-3p expression in pancreatic ductal adenocarcinoma (PDAC) tissue is remarkably lower than that in non-cancerous tissue. Further experiments have shown that miR-193a-3p targets CCND1 to inhibit tumor growth from PDAC cells.[29] In OC, miR-193a-3p regulates GRB7, ERBB4, SOS2, and KRAS expressions in the MAPK/ERK signaling pathway to restrain the proliferation, migration, invasion, and EMT of OC cells.[17] LncRNAs can act as ceRNAs to adsorb miRNAs to reduce their availability.[30] In this work, we demonstrated that DNM3OS is a ceRNA for miR-193a-3p and that DNM3OS negatively regulates miR-193a-3p expression: in OC samples, the expressions of DNM3OS and miR-193a-3p were negatively correlated. We concluded that DNM3OS is highly expressed in OC and contributes to the under-expression of miR-193a-3p. Interestingly, another study has reported that the down-regulation of miR-193a-3p expression in OC is caused by DNA hypermethylation.[17] Our work provides a novel mechanism potentially explaining the dysregulation of miR-193a-3p in OC.

MAP3K3, also known as MEKK3, is a serine/threonine protein kinase of the MAPKs family, which is evolutionarily conservative and expressed in diverse mammalian tissues. Moreover, it acts as a key kinase in different signal transduction cascades and participates in the activation of ERK1/2, p38, JNK, ERK5, NFAT, and NF-κB, which are downstream factors of the MAPK signaling pathway, thereby inducing cell proliferation and differentiation.[31] Accumulating studies suggest that MAP3K3 functions as an oncogene in different types of tumors:[32-36] In breast cancer, MAP3K3 expression is up-regulated, and its high expression predicts an adverse prognosis. MAP3K3 overexpression facilitates cancer cell proliferation, migration, and invasion.[34] In OC, MAP3K3 interacts with Akt and cooperates with Akt to synergistically activate NF-κB signaling, thereby enhancing the chemoresistance of OC cells.[35] Another study has demonstrated that MAP3K3 overexpression reverses the inhibitory effects of miR-212-3p on OC cell proliferation, invasion, and migration.[36] In this work, we validated the binding site between miR-193a-3p and MAP3K3 3'UTR, which was predicted by TargetScan database, and found that miR-193a-3p negatively regulated the expression of MAP3K3. Based on these results, we suggest that MAP3K3 may be a novel target gene of miR-193a-3p. Additionally, we propose that DNM3OS up-regulates MAP3K3 expression by adsorbing miR-193a-3p.

In summary, our study indicates that DNM3OS facilitates OC progression via modulating the miR-193a-3p/MAP3K3 molecular axis. However, there are several limitations in this study. First, the results are based only on in vitro experiments, and therefore, our conclusion must be further validated using in vivo experiments. In addition, whether DNM3OS can enhance other malignant phenotypes of OC cells, such as radioresistance and chemosensitivity, requires further investigation.

ACKNOWLEDGEMENTS

We also thank Hubei Yican Health Industry Co., Ltd. for its linguistic assistance during the preparation of this manuscript.

AUTHOR CONTRIBUTIONS

Conceptualization: all authors. Data curation: all authors. Formal analysis: all authors. Funding acquisition: all authors. Investigation: Lei He. Methodology: Lei He. Project administration: Guolin He. Resources: all authors. Software: Lei He. Supervision: Guolin He. Validation: Guolin He. Visualization: Lei He. Writing—original draft: Lei He. Writing—review & editing: all authors. Approval of final manuscript: all authors.

ORCID iDs

Lei He https://orcid.org/0000-0003-4691-4046
Guolin He https://orcid.org/0000-0003-4950-0586

REFERENCES

1. Lheureux S, Braunstein M, Oza AM. Epithelial ovarian cancer: evolution of management in the era of precision medicine. CA Cancer J Clin 2019;69:280-304.
2. Liu G, Jiang Z, Qiao M, Wang F. Lnc-GIHCG promotes cell proliferation and migration in gastric cancer through miR-1281 adsorption. Mol Genet Genomic Med 2019;7:e711.
3. Ghoneum A, Abdulfattah AY, Said N. Targeting the PI3K/AKT/mTOR/NFκB axis in ovarian cancer. J Cell Immunol 2020;2:68-73.
4. Zong ZH, Du YP, Guan X, Chen S, Zhao Y. CircWHSC1 promotes ovarian cancer progression by regulating MUC1 and hTERT through sponging miR-145 and miR-1182. J Exp Clin Cancer Res 2019;38:437.
5. Ding QS, Zhang L, Wang BC, Zeng Z, Zou XQ, Cao PB, et al. Aberrant high expression level of MORC2 is a common character in multiple cancers. Hum Pathol 2018;76:58-67.
6. Zhou F, Sun Y, Chi Z, Gao Q, Wang H. Long noncoding RNA SNHG12 promotes the proliferation, migration, and invasion of trophoblast cells by regulating the epithelial-mesenchymal transition and cell cycle. J Int Med Res 2020;48:300060520922339.
7. Tu Z, He D, Deng X, Xiong M, Huang X, Li X, et al. An eight-long non-coding RNA signature as a candidate prognostic biomarker for lung cancer. Oncol Rep 2016;36:215-22.
8. Chi Y, Wang D, Wang J, Yu W, Yang J. Long non-coding RNA in the pathogenesis of cancers. Cells 2019;8:1015.
9. Pan L, Meng Q, Li H, Liang K, Li B. LINC00339 promotes cell proliferation, migration, and invasion of ovarian cancer cells via miR-148a-3p/ROCK1 axes. Biomed Pharmacother 2019;120:109423.
10. Li F, Jiang Z, Shao X, Zou N. Downregulation of lncRNA NR2F2 antisense RNA 1 induces G1 arrest of colorectal cancer cells by downregulating cyclin-dependent kinase 6. Dig Dis Sci 2020;65:464-9.
11. Long X, Song K, Hu H, Tian Q, Wang W, Dong Q, et al. Long non-

coding RNA GAS5 inhibits DDP-resistance and tumor progression of epithelial ovarian cancer via GAS5-E2F4-PARP1-MAPK axis. J Exp Clin Cancer Res 2019;38:345.
12. Savary G, Dewaeles E, Diazzi S, Buscot M, Nottet N, Fassy J, et al. The long noncoding RNA DNM3OS is a reservoir of fibromiRs with major functions in lung fibroblast response to TGF-β and pulmonary fibrosis. Am J Respir Crit Care Med 2019;200:184-98.
13. Wang R, Zhang M, Ou Z, He W, Chen L, Zhang J, et al. Long noncoding RNA DNM3OS promotes prostate stromal cells transformation via the miR-29a/29b/COL3A1 and miR-361/TGFβ1 axes. Aging (Albany NY) 2019;11:9442-60.
14. Zhang H, Hua Y, Jiang Z, Yue J, Shi M, Zhen X, et al. Cancer-associated fibroblast-promoted LncRNA DNM3OS confers radioresistance by regulating DNA damage response in esophageal squamous cell carcinoma. Clin Cancer Res 2019;25:1989-2000.
15. Fang X, Tang Z, Zhang H, Quan H. Long non-coding RNA DNM3OS/miR-204-5p/HIP1 axis modulates oral cancer cell viability and migration. J Oral Pathol Med 2020;49:865-75.
16. Mitra R, Chen X, Greenawalt EJ, Maulik U, Jiang W, Zhao Z, et al. Decoding critical long non-coding RNA in ovarian cancer epithelial-to-mesenchymal transition. Nat Commun 2017;8:1604.
17. Chen K, Liu MX, Mak CS, Yung MM, Leung TH, Xu D, et al. Methylation-associated silencing of miR-193a-3p promotes ovarian cancer aggressiveness by targeting GRB7 and MAPK/ERK pathways. Theranostics 2018;8:423-36.
18. Jia W, Dong Y, Tao L, Pang L, Ren Y, Liang W, et al. MAP3K3 overexpression is associated with poor survival in ovarian carcinoma. Hum Pathol 2016;50:162-9.
19. Liu H, Zeng SY, Xie Y, Fei CQ, Sun L. Linc-UBC1 stimulates the metastasis and progression of ovarian cancer via downregulating p53 level. Eur Rev Med Pharmacol Sci 2020;24:1054-61.
20. Yuan D, Zhang X, Zhao Y, Qian H, Wang H, He C, et al. Role of lncRNA-ATB in ovarian cancer and its mechanisms of action. Exp Ther Med 2020;19:965-71.
21. Wu X, Wang Y, Zhong W, Cheng H, Tian Z. The long non-coding RNA MALAT1 enhances ovarian cancer cell stemness by inhibiting YAP translocation from nucleus to cytoplasm. Med Sci Monit 2020;26:e922012.
22. Bai Z, Wu Y, Bai S, Yan Y, Kang H, Ma W, et al. Long non-coding RNA SNGH7 is activated by SP1 and exerts oncogenic properties by interacting with EZH2 in ovarian cancer. J Cell Mol Med 2020;24:7479-89.
23. Hirata M, Asano N, Katayama K, Yoshida A, Tsuda Y, Sekimizu M, et al. Integrated exome and RNA sequencing of dedifferentiated liposarcoma. Nat Commun 2019;10:5683.
24. Mei Z, Huang B, Zhang Y, Qian X, Mo Y, Deng N. Histone deacetylase 6 negatively regulated microRNA-199a-5p induces the occurrence of preeclampsia by targeting VEGFA in vitro. Biomed Pharmacother 2019;114:108805.
25. Wang H, Ji X. SMAD6, positively regulated by the DNM3OS-miR-134-5p axis, confers promoting effects to cell proliferation, migration and EMT process in retinoblastoma. Cancer Cell Int 2020;20:23.
26. Wang S, Ni B, Zhang Z, Wang C, Wo L, Zhou C, et al. Long noncoding RNA DNM3OS promotes tumor progression and EMT in gastric cancer by associating with Snail. Biochem Biophys Res Commun 2019;511:57-62.
27. Zhang L, Liao Y, Tang L. MicroRNA-34 family: a potential tumor suppressor and therapeutic candidate in cancer. J Exp Clin Cancer Res 2019;38:53.
28. Lin YH. MicroRNA networks modulate oxidative stress in cancer. Int J Mol Sci 2019;20:4497.
29. Chen ZM, Yu Q, Chen G, Tang RX, Luo DZ, Dang YW, et al. MiR-193a-3p inhibits pancreatic ductal adenocarcinoma cell proliferation by targeting CCND1. Cancer Manag Res 2019;11:4825-37.
30. Zhou RS, Zhang EX, Sun QF, Ye ZJ, Liu JW, Zhou DH, et al. Integrated analysis of lncRNA-miRNA-mRNA ceRNA network in squamous cell carcinoma of tongue. BMC Cancer 2019;19:779.
31. Zhang Y, Wang SS, Tao L, Pang LJ, Zou H, Liang WH, et al. Overexpression of MAP3K3 promotes tumour growth through activation of the NF-κB signalling pathway in ovarian carcinoma. Sci Rep 2019;9:8401.
32. Santoro R, Zanotto M, Carbone C, Piro G, Tortora G, Melisi D. MEKK3 sustains EMT and stemness in pancreatic cancer by regulating YAP and TAZ transcriptional activity. Anticancer Res 2018;38:1937-46.
33. Tang H, Lv W, Sun W, Bi Q, Hao Y. miR-505 inhibits cell growth and EMT by targeting MAP3K3 through the AKT-NFκB pathway in NSCLC cells. Int J Mol Med 2019;43:1203-16.
34. Yin W, Shi L, Mao Y. MiR-194 regulates nasopharyngeal carcinoma progression by modulating MAP3K3 expression. FEBS Open Bio 2019;9:43-52.
35. Samanta AK, Huang HJ, Le XF, Mao W, Lu KH, Bast RC Jr, et al. MEKK3 expression correlates with nuclear factor kappa B activity and with expression of antiapoptotic genes in serous ovarian carcinoma. Cancer 2009;115:3897-908.
36. Zhang L, Zhang Y, Wang S, Tao L, Pang L, Fu R, et al. MiR-212-3p suppresses high-grade serous ovarian cancer progression by directly targeting MAP3K3. Am J Transl Res 2020;12:875-88.

https://doi.org/10.3349/ymj.2021.62.6.535